Article

Journal of the Brazilian Chemical Society

https://dx.doi.org/10.21577/0103-5053.20240022

*J. Braz. Chem. Soc.* **2024**, *35*, 8, e-20240022, 1-16


# Synthesis and Analysis of Carvacrol-Derived Morita-Baylis-Hillman Adducts as Potential Anticancer Agents

*Aliny P. Vasconcelos,*[a] *Francisco J. S. Xavier,*[b] *Aleff Castro,*[c] *Matheus F. Lima,*[a] *Lucas E. L. Terceiro,*[a] *Fábio P. L. Silva,*[c] *Mario L. A. A. Vasconcellos,*[c] *Bruna B. Dantas,*[d] *Andrezza M. Barbosa,*[a] *Sâmia S. Duarte,*[a] *Demetrius A. M. Araújo*[a] *and Claudio G. Lima-Junior*[*,c]

[a]*Departamento de Biotecnologia, Universidade Federal da Paraíba, 58051-900 João Pessoa-PB, Brazil*

[b]*Instituto Federal de Educação, Ciência e Tecnologia do Rio Grande do Norte, 59360-000 Parelhas-RN, Brazil*

[c]*Laboratório de Síntese Orgânica Medicinal da Paraíba (LASOM-PB), Departamento de Química, Universidade Federal da Paraíba, 58051-900 João Pessoa-PB, Brazil*

[d]*Unidade Acadêmica de Saúde, Centro de Educação e Saúde, Universidade Federal de Campina Grande, 58175-000 Cuité-PB, Brazil*

This study investigates the potential of Morita-Baylis-Hillman adducts derived from carvacrol as anticancer agents. The synthesis process, involving the reaction of aromatic aldehydes with carvacrol acrylate as a Michael acceptor, resulted in stable adducts with impressive yields ranging from 60 to 92%, achieved within a maximum reaction time of 24 h. Through a screening process utilizing 3-(4,5-dimethylthiazol-2-yl)-2,5-diphenyltetrazolium bromide (MTT) test, compound **6**, identified as the acrylate/2-naphthyl adduct, emerged as the most active within the series among twelve compounds tested. Specifically, compound **6** exhibited a remarkably potent impact on neuroblastoma cell lines, particularly SH-SY5Y cells, with half-maximal inhibitory concentration ($IC_{50}$) of 8.7 μM after 72 h (42 times more potent than carvacrol, $IC_{50}$ = 374.1 μM). The exploration of the selectivity index (SI) against normal cell lines demonstrated an outstanding SI of 4.28 compared to other compounds. Mechanistic studies on SH-SY5Y cells revealed a concentration-dependent apoptotic effect attributed to caspase 3/7 activation. *In silico* modeling showcased favorable pharmacokinetic properties for compound **6**, including effective absorption after oral administration. Assessment of toxicity of compound **6** profile using brine shrimp and the Irwin test indicated low toxicity, highlighting its potential for future anticancer agent development.

**Keywords:** Morita-Baylis-Hillman reaction, C–C bond formation, molecular hybridization, apoptosis, neuroblastoma, anticancer activity

## Introduction

Cancer incidence and mortality rates remain a significant global challenge and rank as one of the leading causes of deaths worldwide, representing a major threat to life expectancy. According to the World Health Organization (WHO),[1] cancer is responsible for millions of deaths each year. In 2020, an estimated 10 million cancer-related deaths were reported globally. Additionally, cancer incidence and mortality continue to rise, with the WHO projecting an alarming increase in new cases and mortality in the coming years. Thus, to address the growing number of cancer incidence, it is necessary the development of new treatment strategies to improve patient management and outcome.[1]

The limited effectiveness and lack of selectivity of most chemotherapy options available is one of the main challenges to treat cancer.[2,3] A significant cytotoxicity effect against both cancer and normal cells is strongly associated with the anticancer therapy available.[4] This contributes to the extensive side effects associated with chemotherapy, ultimately impacting the quality of life of patients undergoing cancer treatment.[5,6] As a result, the global scientific community is actively focusing on the development of selective and effective anticancer drugs,

*e-mail: claudio@quimica.ufpb.br
Editor handled this article: Brenno A. D. Neto

emphasizing the important goal of creating effective and precisely targeted medications to combat cancer.[7]

Natural products have gained considerable interest in pharmaceutical chemistry due to their inherent therapeutic attributes.[8] The 2-methyl-5-(propane-2-yl)phenol, also known as carvacrol, is a phenolic monoterpene compound widely found in essential oils derived from oregano (*Origanum vulgare*), thyme (*Thymus vulgaris*), pepperwort (*Lepidium flavum*), wild bergamot (*Citrus aurantium bergamia*), and other plants.[9] This compound has been the subject of extensive research as a promising new candidate for cancer therapy due to its remarkable anticancer activity.[10-15] The effectiveness of carvacrol as an anticancer drug has been demonstrated across various types of cancer, including breast cancer, gliomas, liver cancer, leukemia, and colon cancer.[9,10] In addition, carvacrol's clinical trials have demonstrated its potential to modulate inflammatory processes associated with respiratory disorders like asthma.[16,17] Notably, carvacrol's safety and tolerability have been established through a phase clinical study involving healthy individuals.[18]

The carvacrol molecule has served as the basis for generating innovative cancer-targeting candidates. Through strategic modifications to the structure of carvacrol, including the incorporation of substituents at specific sites, scientists have effectively synthesized derivatives with increased anticancer potential.[11] In this context, a recent study[19] presented the synthesis of a carvacrol-derived copper-Schiff base complex, which showed the ability to suppress dose-dependent proliferation and migration in lung cancer cells, besides creating a mechanism of programmed cell death. This highlights the progress made in improving the effectiveness of carvacrol. Our research group is focused on the development of Morita-Baylis-Hillman adducts (MBHAs) for the organic synthesis of various bioactive compounds.[20-22] Among the various biological activities attributed to MBHAs, their anticancer potential stands out.[23,24]

The Morita-Baylis-Hillman reaction (MBHR) has been extensively utilized in pharmaceutical organic chemistry, which provides a valuable approach for the synthesis of bioactive molecules.[23] This reaction facilitates the formation of chiral centers, resulting in the production of multifunctional cyclic compounds referred to as MBHAs.

Building on previous findings and increasing focus on anticancer drugs, our study sought to synthesize novel carvacrol-derived MBHAs (Figure 1), investigating cytotoxic effects and basic mechanisms of action in neuroblastoma cell lines. Exploring these newly developed compounds, we aim to identify potential new anticancer drugs with significant therapeutic value.

## Results and Discussion

### Synthesis of carvacrol-derived adducts

The chemical reactions for the synthesis of the precursor carvacrol acrylate molecule and the carvacrol-derived adducts (Figure 1), utilizing aromatic aldehydes, were conducted at room temperature using 1,4-diazabicyclo[2,2,2]octane (DABCO) serving as the catalyst, following the procedure previously described by Xavier *et al.*[25] Analysis through thin-layer chromatography (TLC) unveiled the progressive formation of more polar compounds as carvacrol acrylate was consumed during the reaction. This observation indicates the conversion of the aldehyde carbonyl into the adduct hydroxyl, leading to the subsequent formation

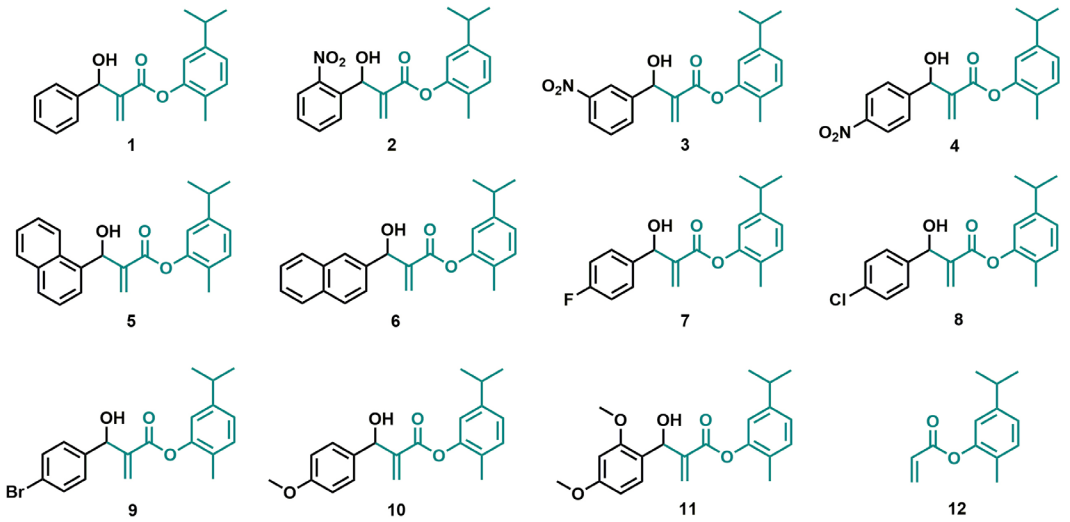


**Figure 1.** Morita-Baylis-Hillman adducts (**1**-**11**) derived from carvacrol acrylate (**12**) synthesized in this work.

of the corresponding MBHA. The comprehensive details regarding the experimental conditions and time required to obtain the racemic hybrids derived from the essential constituent carvacrol (**1-11**) are presented in Table 1.

Nitrate derivatives (*ortho*, *meta* and *para*-nitrobenzaldehydes) are highly reactive against acrylates derived from phenolic monoterpenes, as investigated by our research group.[22,25] Consequently, the reaction times required for the formation of products based on these aldehydes (**2-4**) deviated from the observed pattern for other studied compounds, necessitating a total reaction time of 3 h. In these systems involving nitrated compounds, the formation of very polar co-products was observed, suggesting the occurrence of polymerization reactions. Contrastingly, for the other aldehydes investigated (**1**, **5-11**), the total reaction time was 24 h, resulting in the complete consumption of carvacrol acrylate without the formation of by-products. Overall, the compounds displayed moderate to good yields (Table 1), showcasing stability post-purification and storage.

The Fourier transform infrared (FTIR) spectra of the carvacrol-derived MBHAs (**1-11**) (Supplementary Information section) revealed a distinctive band around 1730 $cm^{-1}$, corresponding to the C=O carbonyl stretching, consistent with the anticipated characteristics of the proposed compounds. Additionally, a broad band within the range of 3600-3200 $cm^{-1}$, attributed to the stretching of the O–H bond introduced in the structure by MBHR, was observed in the FTIR spectra. Clear signals corresponding to the vinylic hydrogens, and the broad singlet indicative of the hydroxyl hydrogen were discernible in the proton nuclear magnetic resonance ($^1$H NMR) spectra, typical features of the MBHA. These results underscore the success of the synthesis, particularly regarding the proposed novel compounds.

Some mechanistic proposals have been described to explain the formation of MBHAs, both in protic and aprotic media. In this work, a polar aprotic solvent (acetonitrile) was used, and the Scheme 1 outlines the mechanistic proposal for the formation of carvacrol-derived MBHAs in this work. In step 1, the occurrence of a 1-4 Michael addition of DABCO to the carvacrol acrylate (Michael acceptor) is proposed, leading to the formation of zwitterionic Intermediate 1. Step 2 involves an aldol condensation between an aldehyde molecule and Intermediate 1, resulting in Intermediate 2. Steps 1 and 2 are the same in protic or aprotic media solvent,[26,27] but the mechanism diverges in step 3 due to prototropism. According to McQuade's proposal,[26] prototropism involves a second aldehyde molecule, leading to the formation of a hemiacetal (step 3). Subsequently, in step 4, an intramolecular proton transfer occurs, followed by the elimination of the DABCO, via

**Table 1.** Reaction time and yield from each MBHA obtained

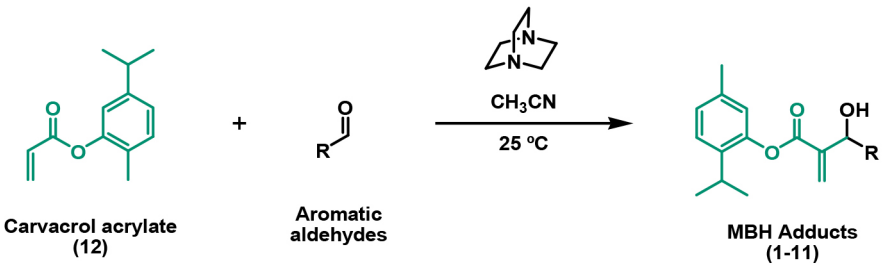


R= Ph; (2-$NO_2$)-Ph; (3-$NO_2$)-Ph;(4-$NO_2$)-Ph; 1-Naphthyl; 2-Naphthyl; (4-F)-Ph; (4-Cl)-Ph; (4-Br)-Ph; (4-MeO)-Ph]; (2,5-*di*MeO)-Ph

| Compound | Aldehyde | Reaction time / h | Yield / % |
|---|---|---|---|
| **1** | benzaldehyde | 24 | 78 |
| **2** | 2-nitrobenzaldehyde | 3 | 72 |
| **3** | 3-nitrobenzaldehyde | 3 | 63 |
| **4** | 4-nitrobenzaldehyde | 3 | 92 |
| **5** | 1-naphthaldehyde | 24 | 71 |
| **6** | 2-naphthaldehyde | 24 | 78 |
| 7 | 4-fluorobenzaldehyde | 24 | 77 |
| **8** | 4-chlorobenzaldehyde | 24 | 85 |
| **9** | 4-bromobenzaldehyde | 24 | 83 |
| **10** | 4-methoxybenzaldehyde | 24 | 60 |
| **11** | 2,5-dimethoxybenzaldehyde | 24 | 65 |

E1cB (step 5). Our contribution to the mechanistic proposal suggests a second consecutive elimination that converts Intermediate 3 to Intermediate 4 (step 6). The balance of positive and negative charges is maintained, and the driving force for elimination would be the ability of oxygen to accept negative charges. The terminal step (step 7) involves the deprotonation of the carbonyl cation, resulting in the restoration of an aldehyde molecule and generating the respective MBHA.

## *In vitro* biological investigation

### Cytotoxic effects of synthetic carvacrol-derived MBHAs in cancer and normal cell lines

The cytotoxicity evaluation of the twelve synthetic carvacrol-derived compounds (**1**-**12**) and carvacrol was conducted through the MTT assay (3-(4,5-dimethylthiazol-2-yl)-2,5-diphenyltetrazolium bromide) on both the human neuroblastoma cancer cell line (SH-SY5Y) and the normal human kidney cell line (HEK-293). The cells were treated with various concentrations of the twelve synthetic compounds and carvacrol for the time of 24 h. The cytotoxic activity of the compounds was determined by the half-maximal inhibitory concentrations ($IC_{50}$) accompanied by the standard error (SE) values, as shown in Table 2 and Figure 2.

Among the tested compounds, eight out of twelve demonstrated cytotoxic activity against the neuroblastoma cell line. Compound **1**, the benzaldehyde derivative, exhibited an $IC_{50}$ value of 30.69 ± 1.11 μM. The nitrate derivatives, including *ortho*, *meta*, and *para*-nitrobenzaldehydes (compounds **2**, **3**, and **4**, respectively), displayed $IC_{50}$ values of 9.79 ± 1.2, 15.94 ± 1.08, and 32.33 ± 1.1 μM, respectively. Compound **6**, the naphthaldehyde derivative, showed an $IC_{50}$ value of 23.36 ± 1.5 μM. The halogen derivatives, namely 4-fluorobenzaldehyde, 4-chlorobenzaldehyde, and 4-bromobenzaldehyde (compounds **7**, **8**, and **9**, respectively), exhibited $IC_{50}$ values of 27.56 ± 1.18, 25.86 ± 1.25, and 25.64 ± 1.26 μM, respectively.

In contrast to the cytotoxic effects of the carvacrol-derived MBHAs on cancer cells, carvacrol itself demonstrated an $IC_{50}$ value of 374.10 ± 1.18 μM, indicating

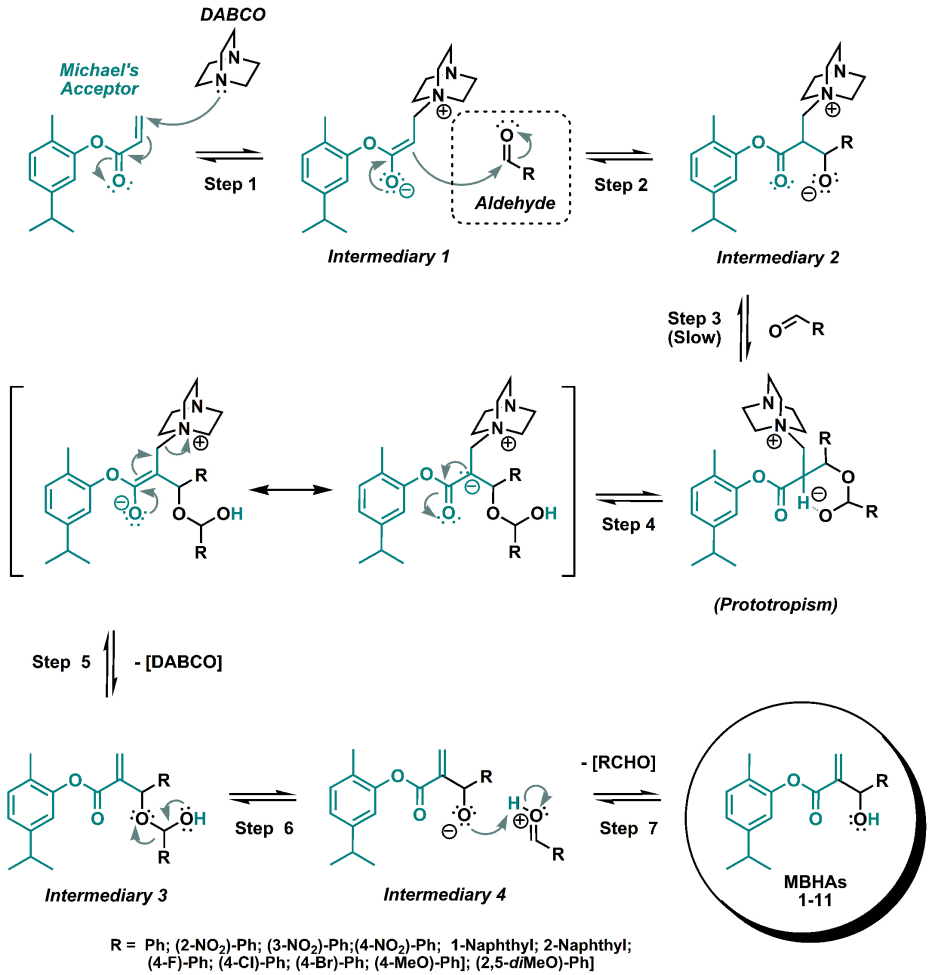


**Scheme 1.** Proposed reaction mechanism, according to McQuade and co-workers.[26]

an anticancer effect that is 10-fold weaker than its synthetic derivatives.

To assess the therapeutic potential of the compounds, we determined the selectivity index (SI) by calculating the quotient of $IC_{50}$ values between normal and cancer cell lines, using the equation: SI = $IC_{50}$ (HEK-293)/ $IC_{50}$ (SH-SY5Y). Higher SI values suggests potential anticancer properties, as they indicate higher $IC_{50}$ values for normal cell lines and lower to cancer cells. Compounds **1**, **4**, and **6** exhibited selectivity indexes greater than three, indicating that their cytotoxic effects were more effective on cancer cells compared to normal cells.

Compound **6** displayed the highest selectivity index within the series of MBHA carvacrol derivatives, with an SI > 4.28. This indicates its enhanced anticancer activity against neuroblastomas. Additionally, compound **1**, containing the benzaldehyde moiety, demonstrated significant cytotoxic effects. Compound **4**, which incorporated the *para*-nitrobenzaldehyde moiety, also exhibited notable anticancer activity when compared to its positional isomers, compounds **2** and **3**, containing the *ortho*-nitrobenzaldehyde and *meta*-nitrobenzaldehyde moieties, respectively.

The use of nitrobenzaldehydes in photodynamic therapy as a light-activation of the $H^+$ carrier induces apoptosis in cancerous and normal cell lines, including breast, prostate, and pancreatic cancers.[28] Remarkably, this approach has demonstrated efficacy in reducing tumor size in mice with triple negative breast cancer, which normally has a poor prognosis.[29]

Compounds featuring a naphthaldehyde moiety, as well as naphthyl chalcones, which has been shown an anticancer property against human acute myeloid leukemia K562 cells and on human acute lymphoblastic leukemia Jurkat cells,[30] have also exhibited a cytotoxic activity against the breast cancer cell line 4T1.[31] Notably, the presence of the 1-naphthaldehyde moiety is a shared characteristic, prominently observed in compound **6**, the most active of the series. Our comparative analysis between compound **6** and its positional isomer, compound **5**, reveals a significant difference in biological impact. Compound **6**, featuring the 1-naphthaldehyde moiety, exhibits substantial biological activity. In contrast, compound **5**, along with compound **11**, demonstrates the lowest biological activity in our study, underscoring the crucial role of structural features in determining biological effects within this compound series.

Several studies have explored the cytotoxic activity of carvacrol on various cancer cell lines including: neuroblastomas,[32] colon cancer,[10] prostate cancer,[33] ovarian cancer,[34] breast cancer,[35] leukemia,[36] etc. Carvacrol has exhibited a significant potential in inhibiting the proliferation of cancer cells and inducing apoptosis.[37] Despite its effectiveness, the selectivity evaluation of carvacrol, as reflected in the results presented in Table 2, yields a SI value of 0.93. These findings reinforce the therapeutic constraints of carvacrol, underscoring the imperative to explore novel therapeutic molecules. Motivated by these insights, we have chosen to delve deeper into the antitumor activity of compound **6**, building upon the precedent set by carvacrol, across a diverse array of cancer cell lines.

**Table 2.** Anticancer activity of the tested compounds is described by half maximal inhibitory concentrations ($IC_{50}$) value (24 h treatment, MTT assay)

| Compound | $IC_{50}$ ± SE[a] / μM | | Selectivity index[b] |
|---|---|---|---|
| | SH-SY5Y (Cancer) | HEK293 (Normal) | |
| **1** | 30.69 ± 1.10 | > 100 | 3.25 |
| **2** | 9.79 ± 1.20 | 14.02 ± 1.16 | 1.43 |
| **3** | 15.94 ± 1.08 | 29.19 ± 1.15 | 1.83 |
| **4** | 32.33 ± 1.10 | > 100 | 3.09 |
| **5** | > 100 | > 100 | ND |
| **6** | 23.36 ± 1.50 | > 100 | 4.28 |
| **7** | 27.56 ± 1.18 | 31.48 ± 1.13 | 1.14 |
| **8** | 25.86 ± 1.25 | 35.05 ± 1.05 | 1.35 |
| **9** | 25.64 ± 1.26 | 35.31 ± 1.03 | 1.37 |
| **10** | 64.72 ± 1.14 | > 100 | 1.54 |
| **11** | > 100 | > 100 | ND |
| **12** | > 50 | > 100 | ND |
| Carvacrol | 374.1 ± 1.18 | 350.1 ±1.04 | 0.93 |

[a]Data was represented as mean $IC_{50}$ value ± SE (standard error) from three independent experiments; [b]calculation of the selectivity index (SI). SI = $IC_{50}$ (normal cell lines)/$IC_{50}$ (cancer cell lines). ND: not determined.

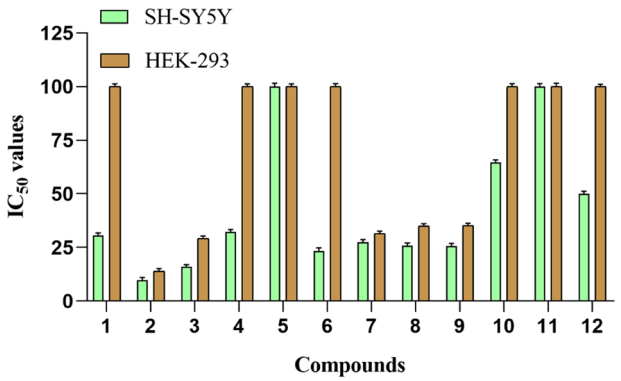


**Figure 2.** Comparison of the $IC_{50}$ values of the carvacrol derivatives in SH-SY5Y and HEK-293, cancer and normal cell lines, respectively. Data was represented as mean $IC_{50}$ value ± SE (standard error) from three independent experiments after 24 h of the compound's incubation.

## Evaluation of the anticancer properties of compound **6**

To further explore the anticancer potential of compound **6**, we conducted the MTT assay in a panel of

different cancer cell lines. Table 3 presents the $IC_{50}$ values of neuroblastoma cell lines (SH-SY5Y, NEURO-2A, KELLY), glioma cell lines (U373MG, U87MG), breast cancer cell line (MCF-7), leukemia monocytic cell line (THP-1), as well as normal cell lines (L929 and HEK-293) after 24 and 72 h of incubation.

Compound **6** demonstrated a significant cytotoxic activity against neuroblastoma cell lines, with a clear dose-dependent and time-dependent response. The $IC_{50}$ values for SH-SY5Y, KELLY, and NEURO-2, after 72 h of incubation were 8.7 ± 2.06, 24.25 ± 1.08, and 12.00 ± 2.79 μM, respectively. This highlights the potent cytotoxic effect of compound **6** on neuroblastoma cells.

In contrast, compound **6** did not exhibit a significant cytotoxic effect on the glioma cell lines, even at higher concentrations tested, suggesting limited efficacy in this cancer type. Similarly, in MCF-7 and THP-1 cell lines, the $IC_{50}$ values exceeded 50 μM after both 24 and 72 h of incubation, indicating lower cytotoxic activity in these cell lines.

Importantly, compound **6** demonstrated a high safety profile as it did not inhibit the viability of normal cell lines HEK-293 and L929, even when used in high concentrations. This underscores its potential as a promising anticancer agent with minimal toxicity to normal cells, along with the selective effect between different cell types-a key attribute in the quest for an ideal therapeutic approach. In contrast, conventional chemotherapeutic agents like doxorubicin and etoposide, routinely employed in daily cancer treatments, induce cytotoxic effects on both normal and tumor cells.[38] This underscores the pressing need for treatments that can effectively distinguish between these distinct cell populations.

**Table 3.** Cytotoxic activity of compound **6** in neuroblastoma (SH-SY5Y; KELLY; NEURO-2A), glioma (U87MG and U37MG), breast cancer (MCF-7), acute monocytic leukemia (THP-1) and non-cancer (HEK-293 and L929) cell lines

| Cell line | Compound **6** $IC_{50}$ ± SE[a] / μM | |
|---|---|---|
| | 24 h | 72 h |
| SH-SY5Y | 23.36 ± 1.05 | 8.7 ± 2.06 |
| KELLY | 29.77 ± 1.13 | 24.25 ± 1.08 |
| NEURO-2A | 26.49 ± 2.56 | 12.00 ± 2.79 |
| U87MG | > 100 | > 100 |
| U373MG | > 100 | > 100 |
| MCF-7 | 58.22 ± 1.04 | 52.87 ± 1.10 |
| THP-1 | 68.99 ± 1.50 | 67.88 ± 1.81 |
| HEK-293 | > 100 | > 100 |
| L929 | > 100 | > 100 |

[a]Data represented as mean half maximal inhibitory concentrations ($IC_{50}$) value ± standard error (S.E.) from three independent experiments.

### Live cell apoptosis analysis

Phosphatidylserine, a marker for cell death, undergoes a translocation from the inner to the outer cell membrane during the apoptosis cascade.[39] Annexin V, a member of the annexin protein group, specifically binds to externalized phosphatidylserine during the apoptotic process. To investigate the cell death mechanism of the carvacrol-derivative MBHA compound **6**, we treated SH-SY5Y cells with 25 μM of the compound for 24 h. Following the treatment, the cells were stained with Hoechst and annexin V, and subsequently visualized using a live cell fluorescence microscope. The number of annexin V positive cells increased following the incubation with compound **6**, indicating the occurrence of apoptosis as the cell death mechanism. The red staining observed in Figure 3, representing annexin V binding, further confirms the occurrence of cell death through apoptosis in SH-SY5Y neuroblastoma cells. For a more comprehensive visualization of the apoptotic process in SH-SY5Y cells after incubation with compound **6**, please refer to the time-lapse video available in the Supplementary Information section.

Furthermore, targeting apoptosis stands out as the most promising non-surgical approach to treating cancer. This strategy is effective across diverse cancer types because evading apoptosis is a common hallmark of cancer, irrespective of its underlying causes or specific type.[40,41] The arsenal of anticancer drugs aimed at intervening in various stages of both the intrinsic and extrinsic apoptosis pathways continues to expand.[14,42,43] As the development of apoptosis-inducing anticancer drugs progresses, ongoing research will determine the most effective targets within these pathways.

### Compound **6** increases caspase 3/7 activity in SH-SY5Y cells

Activation of executioner caspases 3/7 plays a critical role in initiating cellular apoptosis, making it a key component in this process.[44] Caspase-3, normally found in its inactive zymogen form (32KD) in the cytoplasm, can be activated by upstream signaling molecules. Once activated, it targets downstream apoptosis proteins during the early stages of apoptosis, ultimately driving the cell towards programmed cell death.[45] In this study, the impact of compound **6** on cell apoptosis was evaluated using the caspase 3/7 activity apoptosis assay kit CellEvent™, which utilizes a fluorogenic substrate to detect activated caspases 3 and 7 in apoptotic cells.

As shown in Figures 4a-4b, our results demonstrated that compound **6** induces a dose-dependent increase in caspase 3/7 activity in SH-SY5Y cells. This observation

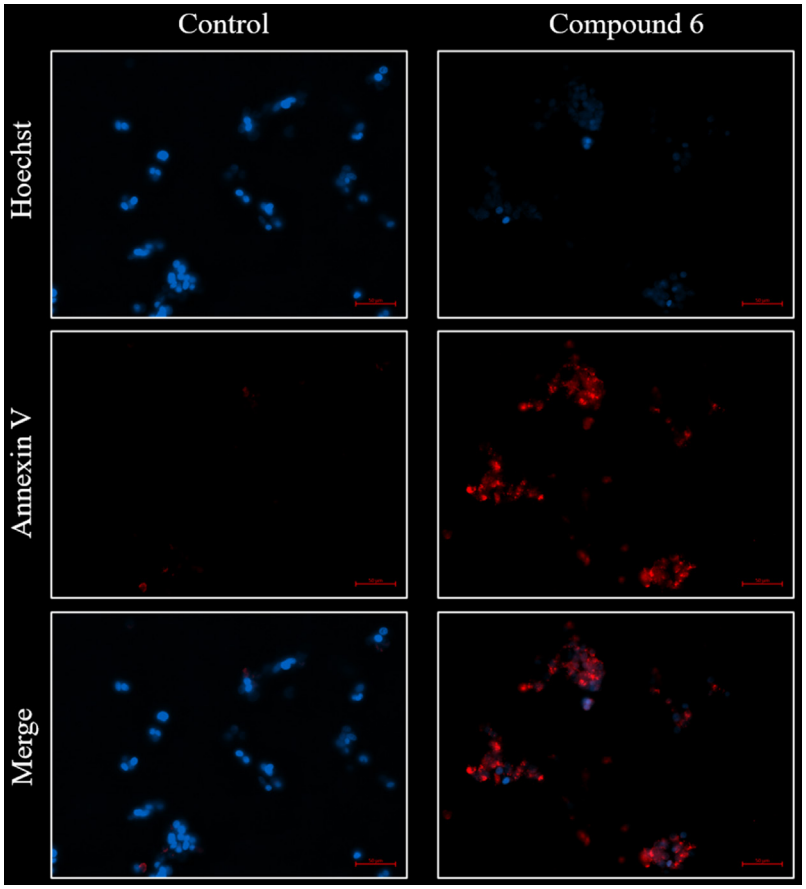


**Figure 3.** DNA staining using Hoechst (blue) and phosphatidylserine staining using annexin V (red) to detect apoptosis SH-SY5Y cells after 24 h incubation with compound **6** (25 μM). Merge is Hoechst staining/annexin V staining overlay. Magnification 400×.

suggests that compound **6** effectively triggers apoptotic pathways in these cells. Notably, the effect of 25 μM compound **6**, corresponding to approximately the $IC_{50}$ value following a 24 h incubation period in SH-SY5Y cells, resulted in approximately 80% of the cells displaying signs of apoptosis. These findings provide valuable insights into the apoptotic potential of compound **6** and highlight its ability to modulate caspase 3/7 activity in SH-SY5Y cells. Further analysis and characterization of compound **6**'s apoptotic mechanisms will contribute to a better understanding of its potential as a therapeutic agent.

### *In silico* ADME (absorption, distribution, metabolism and excretion) studies

Considering the relevance of *in silico* methods as a strategy to accelerate the discovery of possible drugs, we used the SwissADME tool[46] to predict properties of interest in the search for new bioactive compounds. Table 4 presents the results obtained for the Lipinski and Veber's parameters, as well as pharmacokinetic properties based on these physical properties.

The results obtained from the *in silico* approach demonstrate that only the compounds obtained from aldehydes containing naphthyl (**5** and **6**) and 4-halophenyl (**7**-**9**) moieties as substituents exceeded the lipophilicity value predicted by Lipinski's rule (Log $P_{o/w} \leq 4.15$).[47] However, all other Lipinski parameters were respected by carvacrol derivatives **1**-**12**, indicating a class of compounds with good cell membrane permeability and good absorption after oral administration. These compounds also met the requirements of the Veber's parameters, which consider the molecular rigidity, expressed by the number of rotational bonds (≤ 10); and the polar surface area of the molecule (≤ 140 Å$^2$) to predict its oral availability.[48] Concerning the theoretical solubility in water (Log S), MBHAs have moderate solubility compared to carvacrol acrylate (**12**), used as a precursor to obtain the derivatives proposed here. Nitro compounds as well as those with a naphthyl moiety (**2-6**) showed Log S < –6, being slightly more insoluble in water than the other compounds of the proposed series. Allied to intestinal permeability, these data allow a broad categorization of the intestinal absorption potential of these compounds.[49] In the tests presented here, high intestinal absorption (GIA) was verified, in addition to permeability in the blood-brain barrier (BBB). Only nitrated compounds (**2**-**5**)

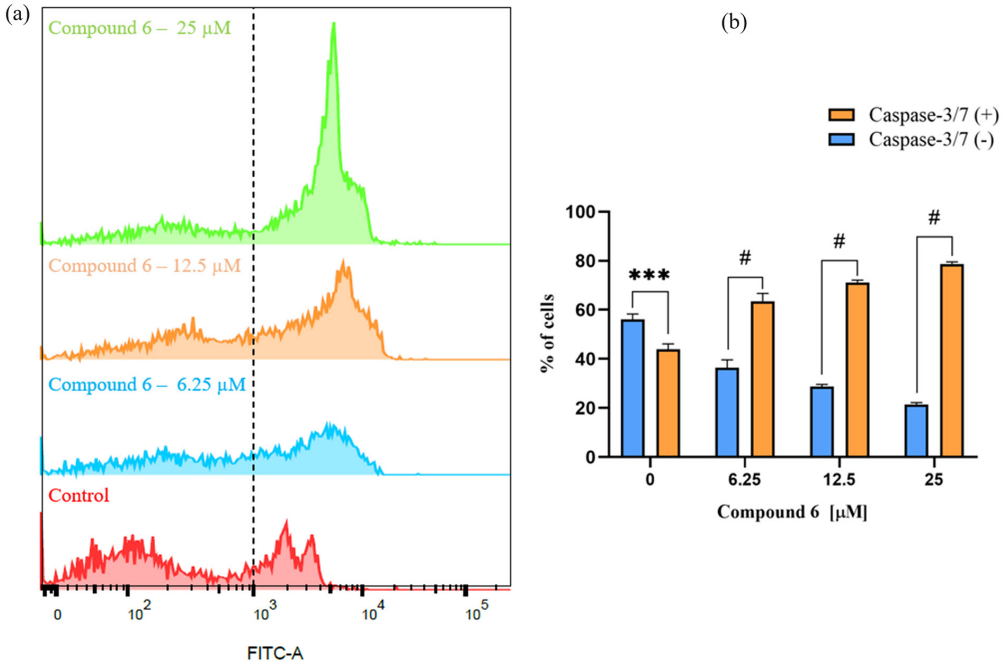


**Figure 4.** Compound **6** induces a dose-dependent activation of caspase 3/7 in SH-SY5Y cells. The neuroblastoma cells were treated with different concentrations of compound **6** (6.25, 12.5, and 25 µm) for 24 h, followed by measurement of caspase 3/7 activity using flow cytometry. Representative flow cytometry histogram (a) and the correspondent percentage of positive and negative cells to caspase 3-7 activation (b) after incubation with compound **6**. Data were analyzed using one-way ANOVA following Tukey's *t*-test. The data are shown as the means ± SD (standard deviation) of three independent experiments. (***$p < 0.001$ and #$p < 0.0001$).

**Table 4.** *In silico* ADME predictions of compounds **1-12** via SwissADME

| Compound | Lipinski's parameters | | | | Veber's parameters | | Log S | GIA | BBB |
|---|---|---|---|---|---|---|---|---|---|
| | MW / (g mol$^{-1}$) | HBA | HBD | Log $P_{o/w}$ | nRB | TPSA / Å$^2$ | | | |
| **1** | 310.39 | 3 | 1 | 3.90 | 6 | 46.53 | –5.27 | high | yes |
| **2** | 355.38 | 5 | 1 | 2.89 | 7 | 92.35 | –6.06 | high | no |
| **3** | 355.38 | 5 | 1 | 2.89 | 7 | 92.35 | –6.06 | high | no |
| **4** | 355.38 | 5 | 1 | 2.89 | 7 | 92.35 | –6.06 | high | no |
| **5** | 360.45 | 3 | 1 | 4.58 | 6 | 46.53 | –6.57 | high | yes |
| **6** | 360.45 | 3 | 1 | 4.58 | 6 | 46.53 | –6.57 | high | yes |
| **7** | 328.38 | 4 | 1 | 4.28 | 6 | 46.53 | –5.37 | high | yes |
| **8** | 344.83 | 3 | 1 | 4.39 | 6 | 46.53 | –5.92 | high | yes |
| **9** | 389.28 | 3 | 1 | 4.50 | 6 | 46.53 | –6.00 | high | yes |
| **10** | 340.41 | 4 | 1 | 3.54 | 7 | 55.76 | –5.44 | high | yes |
| **11** | 370.44 | 5 | 1 | 3.20 | 8 | 64.99 | –5.61 | high | yes |
| **12** | 204.26 | 2 | 0 | 3.31 | 4 | 26.30 | –3.79 | high | yes |
| Carvacrol | 150.22 | 1 | 1 | 2.76 | 1 | 20.23 | –3.60 | high | yes |

MW: molecular weight (≤ 500); HBA: number of H-bond acceptors (≤ 10); HBD: number of H-bond donors (≤ 5); Log $P_{o/w}$: MLog of octanol/water partition coefficient (≤ 4.15);[47] nRB: number of rotatable bonds (≤ 10); TPSA: topological polar surface area (≤ 140 Å$^2$);[48] Log S: Log of solubility calc Ali;[49] GIA: gastrointestinal absorption; BBB: blood brain barrier permeability.

did not show permeability through the BBB. MBHA compound **6** violated the lipophilicity parameter, but this does not compromise the biological results obtained, since the violation of a parameter is commonly accepted, as long as the others are obeyed, without compromising the bioavailability of the drug.[47]

## Toxicology analysis

### Toxicity evaluation of compound **6** on *Artemia salina* nauplii

The high toxicity associated with anticancer compounds currently available in the clinic poses significant limitations on their use, often resulting in reduced patient quality of

life, necessitating dosage adjustments, or even suspension of administration. Consequently, there is a pressing need to explore new therapeutic avenues. In the quest for novel drugs with antitumor properties, the preliminary test to evaluate compound toxicity using *Artemia salina* emerges as a standout method. This test offers substantial advantages, notably its cost-effectiveness and straightforwardness, making it a promising approach in drug development research.[50-54]

In Figure 5, we assessed the toxicity of compounds **6** and **7** on *Artemia salina* nauplii across a concentration range of 0 to 100 µM. Notably, compound **6** exhibited no toxicity at any of the examined concentrations, demonstrating an exceptionally low mortality rate comparable to the negative control DMSO (dimethyl sulfoxide). Conversely, compound **7** triggered mortality starting at the concentration of 50 µM, with a mortality percentage surpassing 80% at the maximum studied concentration of 100 µM. According to our *in vitro* cytotoxic results, among the tested compounds, compound **6** is notably the most intriguing one in the series, displaying the highest SI value. In contrast, compound **7** exhibited one of the lowest SI values. Based on these obtained results, compound **6** stands out among carvacrol derivatives for its low toxicity in this multicellular organism of low complexity. As a result, it emerges as the most promising candidate for further investigations.

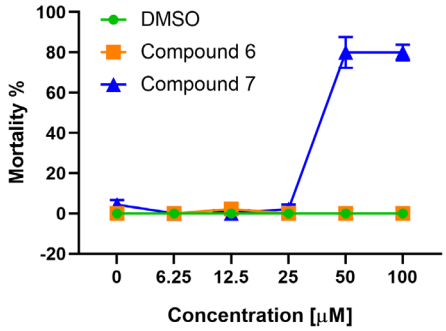


**Figure 5.** Effect of carvacrol derivatives **6** and **7**, along with the negative control DMSO, on the mortality rate of *Artemia salina* after 24 h of incubation.

### The Irwin test

The use of behavioral techniques in safety pharmacology has grown out of the original comprehensive observational procedure for mice described by Irwin[55] which subsequently provided a basis for prioritizing compounds in the drug discovery process.[56] Nowadays, new chemical compounds can be systematically evaluated for their effects on the nervous system at various doses through behavioral screening. This process aids in identifying potential therapeutic applications and determining suitable doses for further assessments.

In this study, we conducted the Irwin test to explore the impact of compound **6** in behavioral pharmacological screening. Mice were administered two distinct oral doses of compound **6**, namely 65 and 128 mg $kg^{-1}$. Figure 6 delivers a comprehensive presentation of the results, encompassing analyzed parameters for different groups, including the negative control (DMSO) and the two doses of compound **6**. The results demonstrated that no significant behavioral changes were observed in the mice across all the tested groups. Additionally, there were no indications of neurotoxic effects caused by compound **6** at the administered doses. Therefore, based on the experimental outcomes derived from the Irwin test, it can be concluded that compound **6** is not neurotoxic at the tested doses.

## Conclusions

In summary, our study synthesized 11 MBHAs and a carvacrol-derived acrylate labeled as compounds **1**-**12**. Among them, compound **6** exhibited the most favorable selectivity index against the SH-SY5Y neuroblastoma cell line, while displaying a relatively lower cytotoxicity effect towards normal cell lines. Our findings strongly indicate that compound **6** induces a significant apoptotic effect on SH-SY5Y cells in a concentration-dependent manner. Furthermore, compound **6** exhibited lower toxicity in *Artemia salina* and mice. However, additional mechanistic studies and *in vivo* experiments are necessary to validate and translate the observed anticancer properties of compound **6** into potential clinical applications.

## Experimental

### General

All commercially available reagents and solvents were used without further purification. Reactions were monitored by TLC using Silica gel 60 UV254 pre-coated silica gel plates (Macherey-Nagel, Bethlehem, USA) with detection using an UV lamp. Flash column chromatography was performed on 300-400 mesh silica gels. Organic layers were dried over anhydrous $MgSO_4$ or $Na_2SO_4$ (Sigma-Aldrich, St. Louis, USA) and prior to evaporation using a rotary evaporator. $^1$H NMR and $^{13}$C NMR spectra were recorded using a Mercury Spectra AC 20 spectrometer (200 MHz for $^1$H, 50 MHz for $^{13}$C) (Varian, Palo Alto, USA). Chemical shifts were reported relative to internal tetramethylsilane ($\delta$ 0.00 ppm) for $^1$H, using $CDCl_3$ (Cambridge Isotope Laboratories, Tewksbury, USA) as the solvent. FTIR spectra were recorded using a model IR Prestige-21 spectrophotometer (Shimadzu, Kyoto, Japan) in KBr

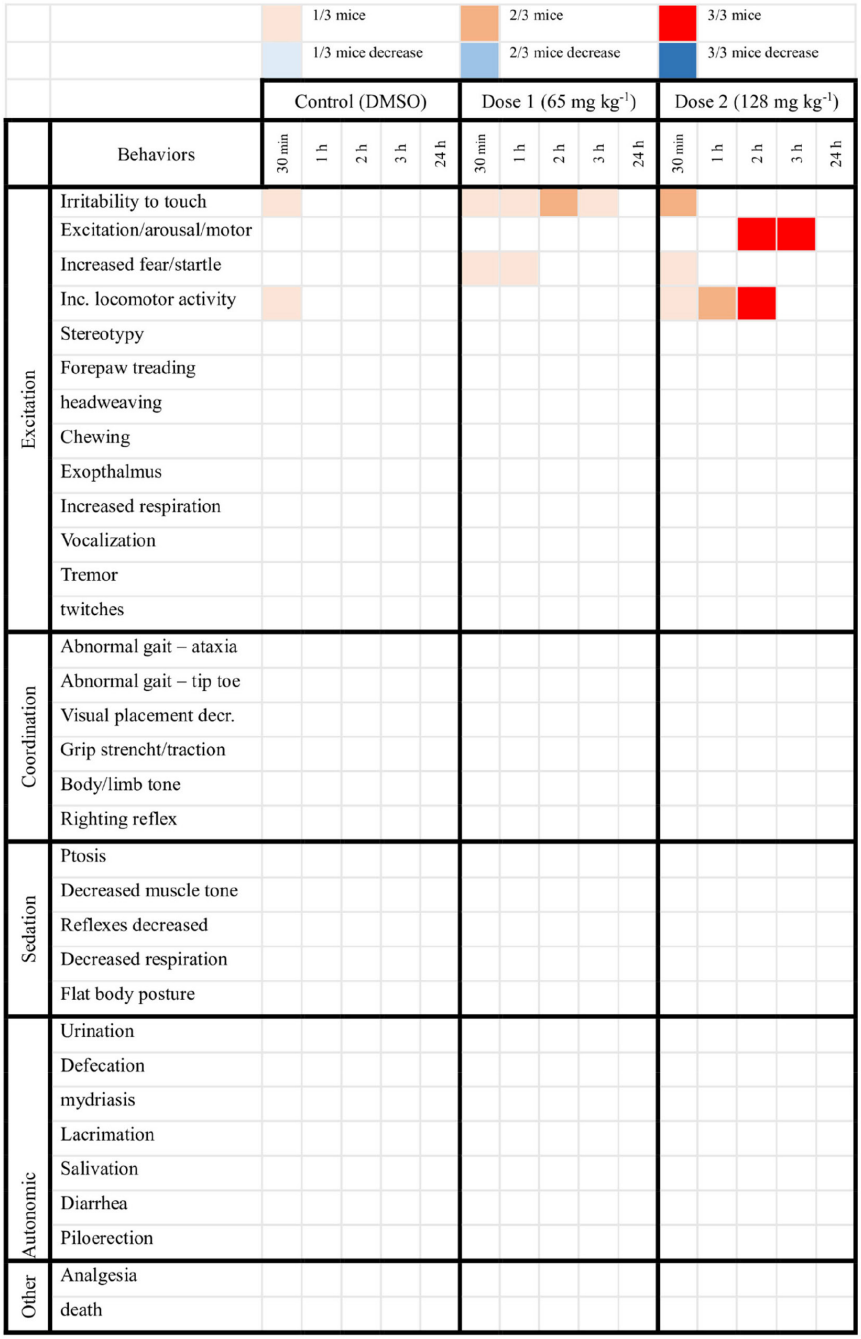


**Figure 6.** Heat map illustrating behaviors induced by compound **6**. Behaviors are categorized into sections such as excitation, coordination, sedation, autonomic, and others. The columns represent different dosage groups (65 and 128 mg $kg^{-1}$) and the timing of observations (30 min, 1, 2, 3, and 24 h). The color intensity in the heat map reflects the number of mice affected at each dose and time. The lightest color corresponds to 1 out of 3 mice, while the darkest color indicates 3 out of 3 mice exhibiting the specific behavior. The red color family signifies an increase in the mentioned behavior, while the blue color family represents a decrease in the observed behavior.

pellets (Sigma-Aldrich, São Paulo, Brazil). High-resolution mass spectra (HRMS) of new hybrids (compounds **3** and **7**-**13**), were obtained using a Q-Tof quadrupole/orthogonal instrument (Waters, Milford, USA). Direct injection acid medium: positive ionization mode, spray ionization with voltage of 3500 V, with a source temperature of 80 °C and a cone voltage of 30 V. The molecules were analyzed at a concentration of 50 μM, in 50% methanol and 0.1% formic acid, injected for 1 min at 2 μL $min^{-1}$. Direct injection basic medium: negative ionization mode, spray ionization using 2500 V, with a source temperature of 80 °C and cone voltage of 20 V. The molecules were analyzed at a concentration of 50 μM, in 50% methanol and 100 mM ammonium bicarbonate, injected for 1 min

at 2 μL $min^{-1}$. Data acquisition and instrument control were conducted using the MassLynx program (version 4.1, Waters, Milford, USA). Mass spectra were acquired with a range of 50-1000 mass/charge ratio (*m/z*), using intervals of 1 s *per* scan applied throughout the acquisition time. The accuracy of the measurements was guaranteed using the Q-Tof LockSpray™ system (Waters, Milford, USA) for calibration.

### Typical procedure for the synthesis of carvacrol-derived MBHAs (**1-11**)

In a reaction flask, 0.5 mmol of carvacrol acrylate (102 mg),[25] 0.6 mmol of the aromatic aldehydes (Sigma-Aldrich, São Paulo, Brazil) and 0.5 mmol of 1,4-diazabicyclo(2,2,2)octane (56 mg) (DABCO; Sigma-Aldrich, São Paulo, Brazil) were solubilized in 1 mL of dry acetonitrile (Tedia, Fairfield, USA). The mixture was stirred at room temperature until conversion to the product. Total conversion was evidenced by TLC and the products (**1**-**11**) were purified with flash chromatography using silica gel and ethyl acetate/hexane (Vetec, Rio de Janeiro, Brazil) as eluent. After evaporation of the solvent under vacuum, the yellow oils obtained were characterized.[25] All MBHAs were obtained as racemic mixtures, and their spectra are available in the Supplementary Information section.

### 5-Isopropyl-2-methylphenyl 2-(hydroxy(phenyl)methyl) acrylate (compound **1**)

78% yield; $^1$H NMR (200 MHz, $CDCl_3$) $\delta$ 7.45-7.28 (m, 5H, H-Ar), 7.01 (dd, *J* 7.8, 4.6 Hz, 2H, H-Ar), 6.74 (d, *J* 1.1 Hz, 1H, H-Ar), 6.57 (s, 1H, H-C-OH), 6.05 (s, 1H, $CH_2$=C), 5.64 (s, 1H, $CH_2$=C), 2.82 (dt, *J* 13.8, 6.9 Hz, 2H, HO-C and HC-$(CH_3)_2$), 1.88 (s, 3H, $H_3$C-Ph), 1.19 (d, *J* 6.9 Hz, 6H, $(CH_3)_2$-CH); $^{13}$C NMR (50 MHz, $CDCl_3$) $\delta$ 162.1, 146.4, 145.6, 139.3, 138.7, 128.4, 126.0, 125.5, 124.8, 124.6, 124.4, 121.8, 117.1, 70.6, 31.0, 21.4, 13.0; IR (KBr) ν / $cm^{-1}$ 3458 (O–H, stretching), 1730 (C=O, stretching), 1625 (C=C, vinyl), 1500 (C=C, aromatic ring stretching); HRMS *m/z*, calcd. $C_{20}H_{22}O_3$ $[M + Na]^+$: 333.1461, found: 333.1514.

### 5-Isopropyl-2-methylphenyl 2-(hydroxy(2-nitrophenyl) methyl)acrylate (compound **2**)

72% yield; $^1$H NMR (200 MHz, $CDCl_3$) $\delta$ 7.87 (dd, *J* 7.1, 7.5 Hz, 2H, H-Ar), 7.62 (t, *J* 7.5 Hz, 1H, H-Ar), 7.42 (t, *J* 7,7 Hz, 1H, H-Ar), 7.03 (dd, *J* 7.6, 7.8 Hz, 2H, H-Ar), 6.81 (s, 1H, H-Ar), 6.58 (s, 1H, H-C-OH), 6.30 (s, 1H, $CH_2$=C), 5.86 (s, 1H, $CH_2$=C), 3.82 (s, 1H, HO-C), 2.99-2.67 (m, 1H, HC-$(CH_3)_2$), 1.96 (s, 3H, $H_3$C-Ph), 1.19 (d, *J* 6.9 Hz, 6H, $(CH_3)_2$-CH); $^{13}$C NMR (50 MHz, $CDCl_3$) $\delta$ 164.4, 148.9, 148.1, 140.8, 136.4, 133.6, 130.9, 129.0, 128.8, 127.7, 127.7, 127.18, 124.8, 124.3, 119.6, 67.5, 33.5, 23.9, 15.6; IR (KBr) ν / $cm^{-1}$ 3489 (O–H, stretching), 1734 (C=O, stretching),1624 (C=C, vinyl), 1527 and 1348 ($NO_2$, axial deformations); HRMS *m/z*, calcd. $C_{20}H_{21}NO_5$ $[M + Na]^+$: 378.1312, found: 378.1374.

### 5-Isopropyl-2-methylphenyl 2-(hydroxy(3-nitrophenyl) methyl)acrylate (compound **3**)

63% yield; $^1$H NMR (200 MHz, $CDCl_3$) $\delta$ 8.30 (s, 1H, H-Ar), 8.15 (dd, *J* 8.2, 1.1 Hz, 1H, H-Ar), 7.79 (d, *J* 7,7 Hz, 1H, H-Ar), 7.53 (t, *J* 7.9 Hz, 1H, H-Ar), 7.06 (dd, *J* 7.2, 7.8 Hz, 2H, H-Ar), 6.79 (s, 1H, H-Ar), 6.68 (s, 1H, H-C-OH), 6.13 (s, 1H, $CH_2$=C), 5.74 (d, *J* 5.2 Hz, 1H, $CH_2$=C), 3.36 (d, *J* 5.6 Hz, 1H, HO-C), 2.97-2.71 (m, 1H, HC-$(CH_3)_2$), 1.95 (s, 3H, $H_3$C-Ph), 1.20 (d, *J* 6.9 Hz, 6H, $(CH_3)_2$-CH); $^{13}$C NMR (50 MHz, $CDCl_3$) $\delta$ 164.3, 148.7, 148.3, 143.6, 140.8, 132.9, 131.0, 129.4, 128.4, 128.3, 1267.0, 124.5, 122.9, 121.6, 119.5, 72.2, 33.5, 23.9, 15.6; IR (KBr) ν / $cm^{-1}$ 3450 (O–H, stretching), 1735 (C=O, stretching),1637 (C=C, vinyl), 1602 (C=C, aromatic ring stretching), 1531 and 1350 ($NO_2$, axial deformations); HRMS *m/z*, calcd. $C_{20}H_{21}NO_5$ $[M + Na]^+$: 378.1312, found: 378.1355.

### 5-Isopropyl-2-methylphenyl 2-(hydroxy(4-nitrophenyl) methyl)acrylate (compound **4**)

92% yield; $^1$H NMR (200 MHz, $CDCl_3$) $\delta$ 8.20 (d, *J* 8.8 Hz, 2H, H-Ar), 7.63 (d, *J* 8.6 Hz, 2H, H-Ar), 7.06 (dd, *J* 7.4, 7.8 Hz, 2H, H-Ar), 6.78 (d, *J* 1.2 Hz, 1H, H-Ar), 6.67 (s, 1H, H-C-OH), 6.12 (s, 1H, $CH_2$=C), 5.75 (d, *J* 4.8 Hz, 1H, $CH_2$=C), 3.50 (d, *J* 4.9 Hz, 1H, HO-C), 2.85 (hept, *J* 6.8 Hz, 1H, HC-$(CH_3)_2$), 1.95 (s, 3H, $H_3$C-Ph), 1.20 (d, *J* 6.9 Hz, 6H, $(CH_3)_2$-CH); $^{13}$C NMR (50 MHz, $CDCl_3$) $\delta$ 164.2, 148.6, 148.3, 147.5, 140.9, 131.0, 128.2, 128.2, 127.6, 127.0, 124.5, 123.6,119.5, 72.4, 33.5, 23.8, 15.6; IR (KBr) ν / $cm^{-1}$ (O–H, stretching), 1728 (C=O, stretching), 1624 (C=C, vinyl), 1606 (C=C, aromatic ring stretching), 1521 and 1348 ($NO_2$, axial deformations); HRMS *m/z*, calcd. $C_{20}H_{21}NO_5$ $[M + Na]^+$: 378.1312, found: 378.1360.

### 5-Isopropyl-2-methylphenyl 2-(hydroxy(naphthalen-1-yl) methyl)acrylate (compound **5**)

71% yield; $^1$H NMR (200 MHz, $CDCl_3$) $\delta$ 7.88-7.74 (m, 4H, H-Ar), 7.47 (m, 3H, H-Ar), 7.00 (dd, *J* 8.2, 7.8 Hz, 2H, H-Ar), 6.71 (s, 1H, H-Ar), 6.62 (s, 1H, H-C-OH), 6.08 (s, 1H, $CH_2$=C), 5.82 (s, 1H, $CH_2$=C), 3.24 (s, 1H, HO-C), 2.79 (dt, *J* 13.8, 6.9 Hz, 1H, HC-$(CH_3)_2$), 1.87 (s, 3H, $H_3$C-Ph), 1.15 (d, *J* 6.9 Hz, 6H, $(CH_3)_2$-CH); $^{13}$C NMR (50 MHz, $CDCl_3$) $\delta$ 165.1, 149.0, 148.1, 141.7, 136.4, 133.9, 130.9, 130.8, 128.8, 128.2, 128.1, 127.2, 126.4, 125.8, 125.4,

124.6, 124.3, 123.7, 119.6, 69.3, 33.5, 23.9, 15.6; IR (KBr) ν / $cm^{-1}$ 3440 (O–H, stretching), 1734 (C=O, stretching), 1625 (C=C, vinyl), 1508 (C=C, aromatic ring stretching); HRMS *m/z*, calcd. $C_{24}H_{24}O_3$ $[M + Na]^+$: 383.1618, found: 383.1652.

5-Isopropyl-2-methylphenyl 2-(hydroxy(naphthalen-2-yl) methyl)acrylate (compound **6**)

78% yield; $^1H$ NMR (200 MHz, $CDCl_3$) $\delta$ 7.92-7.74 (m, 4H, H-Ar), 7.47 (dd, *J* 7.0, 6.7 Hz, 3H, H-Ar), 7.00 (dd, *J* 8.8, 7.8 Hz, 2H, H-Ar), 6.71 (s, 1H, H-Ar), 6.62 (s, 1H, H-C-OH), 6.08 (s, 1H, $CH_2$=C), 5.82 (s, 1H, $CH_2$=C), 3.24 (s, 1H, HO-C), 2.79 (dt, *J* 13.8, 6.9 Hz, 1H, HC-$(CH_3)_2$), 1.87 (s, 3H, $H_3C$-Ph), 1.15 (d, *J* 6.9 Hz, 6H, $(CH_3)_2$-CH); $^{13}C$ NMR (50 MHz, $CDCl_3$) $\delta$ 164.7, 148.9, 148.1, 141.8, 138.6, 133.3, 133.1, 130.9, 128.4, 128.2, 127.7, 127.4, 127.2, 126.2, 126.2, 125.9, 124.7, 124.3, 119.6, 73.3, 33.5, 23.9, 15.6; IR (KBr) ν / $cm^{-1}$ 3450 (O–H, stretching), 1734 (C=O, stretching), 1624 (C=C, vinyl), 1506 (C=C, aromatic ring stretching); HRMS *m/z*, calcd. $C_{24}H_{24}O_3$ $[M + Na]^+$: 383.1618, found: 383.1632.

5-Isopropyl-2-methylphenyl 2-((4-fluorophenyl)(hydroxy) methyl)acrylate (compound **7**)

77% yield; $^1H$ NMR (200 MHz, $CDCl_3$) $\delta$ 7.39 (dd, *J* 8.6, 5.4 Hz, 2H, H-Ar), 7.16-6.94 (m, 4H, H-Ar), 6.75 (s, 1H, H-Ar), 6.59 (s, 1H, H-C-OH), 6.06 (s, 1H, $CH_2$=C), 5.64 (s, 1H, $CH_2$=C), 3.35-2.69 (m, 2H, HO-C and HC-$(CH_3)_2$), 1.91 (s, 3H, $H_3C$-Ph), 1.20 (d, *J* 6.9 Hz, 6H, $(CH_3)_2$-CH); $^{13}C$ NMR (50 MHz, $CDCl_3$) $\delta$ 164.9, 164.5, 160.0, 148.8, 148.2, 141.7, 137.0, 134.0, 131.0, 128.7, 128.5, 127.1, 124.4, 119.6, 115.6, 115.1, 72.5, 33.5, 23.9, 15.5; IR (KBr) ν / $cm^{-1}$ 3456 (O–H, stretching), 1739 (C=O, stretching),1624 (C=C, vinyl), 1602 (C=C, aromatic ring stretching), 1147 (C–F, stretching); HRMS *m/z*, calcd. $C_{20}H_{21}FO_3$ $[M + Na]^+$: 351.1367, found: 351.1427.

5-Isopropyl-2-methylphenyl 2-((4-chlorophenyl)(hydroxy) methyl)acrylate (compound **8**)

85% yield; $^1H$ NMR (200 MHz, $CDCl_3$) $\delta$ 7.37-7.19 (m, 4H, H-Ar), 7.14-6.94 (m, 2H, H-Ar), 6.75 (s, 1H, H-Ar), 6.59 (s, 1H, H-C-OH), 6.05 (s, 1H, $CH_2$=C), 5.62 (s, 1H, $CH_2$=C), 3.21 (s, 1H, HO-C), 2.95-2.72 (m, 1H, HC-$(CH_3)_2$), 1.92 (s, 3H, $H_3C$-Ph), 1.20 (d, *J* 6.9 Hz, 6H, $(CH_3)_2$-CH); $^{13}C$ NMR (50 MHz, $CDCl_3$) $\delta$ 164.5, 148.8, 148.2, 141.5, 139.8, 133.8, 1301.0, 128.7, 128.2, 127.4, 127.1, 124.4, 119.6, 72.5, 33.5, 23.9,15.6; IR (KBr) ν / $cm^{-1}$ 3197 (O–H, stretching), 1737 (C=O, stretching), 1631 (C=C, vinyl), 1597 (C=C, aromatic ring stretching), 1147 (C–Cl, stretching); HRMS *m/z*, calcd. $C_{20}H_{21}ClO_3$ $[M + Na]^+$: 367.1071, found: 367.1084.

5-Isopropyl-2-methylphenyl 2-((4-bromophenyl)(hydroxy) methyl)acrylate (compound **9**)

83% yield; $^1H$ NMR (200 MHz, $CDCl_3$) $\delta$ 7.47 (d, *J* 8.4 Hz, 2H, H-Ar), 7.28 (d, *J* 8.4 Hz, 2H, H-Ar), 7.03 (d, *J* 7.9, 2H, H-Ar), 6.75 (s, 1H, H-Ar), 6.59 (s, 1H, H-C-OH), 6.05 (s, 1H, $CH_2$=C), 5.60 (s, 1H, $CH_2$=C), 3.30 (s, 1H, HO-C), 2.84 (dt, *J* 13.8, 6.9 Hz, 1H, HC-$(CH_3)_2$), 1.92 (s, 3H, $H_3C$-Ph), 1.20 (d, *J* 6.9 Hz, 6H, $(CH_3)_2$-CH); $^{13}C$ NMR (50 MHz, $CDCl_3$) $\delta$ 164.5, 148.8, 148.2, 141.4, 140.3, 131.6, 131.0, 128.6, 127.4, 127.1, 124.4, 121.9, 119.6, 72.5, 33.5, 23.9,15.6; IR (KBr) ν / $cm^{-1}$ 3197 (O–H, stretching), 1737 (C=O, stretching), 1625 (C=C, vinyl), 1591 (C=C, aromatic ring stretching), 1147 (C–Br, stretching); HRMS *m/z*, calcd. $C_{20}H_{21}BrO_3$ $[M + Na]^+$: 411.0572, found: 413.0600.

5-Isopropyl-2-methylphenyl 2-(hydroxy(4-methoxyphenyl) methyl)acrylate (compound **10**)

60% yield; $^1H$ NMR (200 MHz, $CDCl_3$) $\delta$ 7.35 (d, *J* 8.1 Hz, 2H, H-Ar), 7.13-6.73 (m, 5H, H-Ar), 6.58 (s, 1H, H-C-OH), 6.07 (s, 1H, $CH_2$=C), 5.64 (s, 1H, $CH_2$=C), 3.80 (s, 3H, $H_3CO$-Ph), 3.03-2.59 (m, 2H, HO-C and HC-$(CH_3)_2$), 1.92 (s, 3H, $H_3C$-Ph), 1.20 (d, *J* 6.8 Hz, 6H, $(CH_3)_2$-CH); $^{13}C$ NMR (50 MHz, $CDCl_3$) $\delta$ 164.63, 159.37, 148.88, 148.09, 141.94, 133.35, 130.88,128.1, 127.2, 126.7, 124.3, 119.6, 113.9, 72.8, 33.5, 23.9, 15.6; IR (KBr) ν / $cm^{-1}$ 3462 (O–H, stretching), 1735 (C=O, stretching), 1610 (C=C, vinyl), 1585 (C=C, aromatic ring stretching), 1033 (C–O–C, symmetric stretching); HRMS *m/z*, $C_{21}H_{24}O_4$calcd. $[M + Na]^+$: 363.1567, found: 363.1577.

5-Isopropyl-2-methylphenyl 2-((2,4-dimethoxyphenyl) (hydroxy) methyl)acrylate (compound **11**)

78% yield; $^1H$ NMR (200 MHz, $CDCl_3$) $\delta$ 7.17-6.97 (m, 3H, H-Ar), 6.83 (s, 3H, H-Ar), 6.58 (s, 1H, H-C-OH), 5.96 (s, 2H, $CH_2$=C), 3.78 (d, *J* 7.0 Hz, 6H, $H_3CO$-Ph), 3.49 (s, 1H, HO-C), 2.96-2.76 (m, 1H, HC-$(CH_3)_2$), 2.02 (s, 3H, $H_3C$-Ph), 1.22 (d, *J* 6.9 Hz, 6H, $(CH_3)_2$-CH); $^{13}C$ NMR (50 MHz, $CDCl_3$) $\delta$ 164.9, 153.8, 151.0, 149.0, 148.1, 141.2, 130.9, 130.1, 127.3, 127.0, 124.2, 119.7, 113.7, 113.7, 111.9, 68.2, 56.0, 55.8 33.5, 23.9, 15.6; IR (KBr) ν / $cm^{-1}$ 3475 (O–H, stretching), 1735 (C=O, stretching), 1622 (C=C, vinyl), 1589 (C=C, aromatic ring stretching), 1041 (C–O–C, symmetric stretching); HRMS *m/z*, calcd. $C_{22}H_{26}O_5$ $[M + Na]^+$: 393.1672, found: 393.1678.

5-Isopropyl-2-methylphenyl acrylate (compound **12**)

76% yield; $^1H$ NMR (200 MHz, $CDCl_3$) $\delta$ 7.08 (d, *J* 7.6, Hz, 2H, H-Ar), 6.69 (s, 1H, H-Ar), 6.57 (dd, *J* 17.2, 1.4 Hz, 1H, $CH_2$=CH), 6.33 (dd, *J* 17.3, 10.3 Hz, 1H, CH=$CH_2$), 5.97 (d, *J* 10.3 Hz, 1H, $CH_2$=CH), 2.98-2.75 (m,

1H, HC-$(CH_3)_2$), 2.13 (s, 3H, $H_3C$-Ph), 1.23 (d, *J* 6.9 Hz, 6H, $(CH_3)_2$-CH); $^{13}C$ NMR (50 MHz, $CDCl_3$) $\delta$ 164.4, 149.1, 148.1, 132.4, 131.0, 127.9, 127.2, 124.2, 119.7, 33.6, 24.0, 15.8; IR (KBr) $\nu$ / $cm^{-1}$ 1743 (C=O, stretching), 1635 (C=C, acrylic and vinylic groups),1622 (C=C, aromatic ring stretching); HRMS *m/z*, calcd. $C_{13}H_{16}O_2$ $[M + Na]^+$: 227.1043, found: 227.1063.

## Biology

### Cell cultures

The following cell lines were obtained from the Rio de Janeiro Cell Bank (Brazil): SH-SY5Y and KELLY (human neuroblastoma), Neuro-2A (mouse neuroblastoma), U87MG and U373MG (human glioma), MCF-7 (human breast cancer), THP-1 (human leukemia monocytic), HEK-293 (human embryonic kidney), and L929 (mouse fibroblast). For culture purposes, the SH-SY5Y, KELLY, Neuro-2A, U87MG, and U373MG cell lines were maintained in Dulbecco's modified eagle medium (DMEM) high glucose medium (Gigco™ Life Technologies, Gaithersburg, USA). The medium was supplemented with 1% Glutamax (Gigco™ Life Technologies, Gaithersburg, USA), 1% non-essential amino acids, 10% fetal bovine serum (Sigma-Aldrich, St. Louis, USA), and 1% antibiotics (100 U $mL^{-1}$ of penicillin and 100 µg $mL^{-1}$ of streptomycin) (Gigco™ Life Technologies, Gaithersburg, USA). On the other hand, the THP-1, HEK-293, and L929 cell lines were cultured in Roswell Park Memorial Institute (RPMI) medium supplemented with 10% FBS and 1% antibiotics (100 U $mL^{-1}$ of penicillin and 100 µg $mL^{-1}$ of streptomycin). All the cell lines were cultured in a humidified incubator with 5% $CO_2$ at 37 °C.

### Cytotoxicity assay

Cell viability was assessed using the MTT assay, which measures the mitochondrial-dependent reduction of MTT, 3-(4,5-dimethyl2-thiazolyl)-2,5-diphenyl-2*H*-tetrazolium bromide (MTT; Sigma-Aldrich, St. Louis, USA), to a colored blue formazan. Briefly, cells ($3 \times 10^4$ in 100 µL) were seeded in triplicate into a 96-well plate. Following a 24 h culture at 37 °C, the cells were exposed to increasing concentrations of compound **6** or carvacrol for 24 to 72 h. For the negative control, drug-free medium was used, and the solvent control contained the equivalent volume of dimethyl sulfoxide (DMSO; Sigma-Aldrich, St. Louis, USA). After the time exposure, MTT (5 mg $mL^{-1}$) was added, and the plates were further incubated at 37 °C for 4 h. The resulting MTT formazan crystals were dissolved overnight in 100 µL of 10% SDS in 0.01 N HCl (Sigma-Aldrich, St. Louis, USA), and the absorbance was measured at 570 nm using a microplate reader (Biotek Instruments EL800, USA). Cytotoxicity was determined by calculating the $IC_{50}$ value, which represents the concentration that inhibits 50% of cell growth, based on the concentration-response curve obtained (6.25, 12.5, 25.0, 50.0, and 100.0 µM).

### Cell apoptosis analysis

To investigate the apoptotic effect of compound **6** in neuroblastoma cells, SH-SY5Y cells were cultured in chambered coverslips with eight individual wells (Ibidi®, Gräfelfing, Germany). A concentration of 25 µM of compound **6** was added to the test wells, while an equal volume of DMSO was added to the negative control wells. For annexin V staining without the need for washing steps, fluorescently labeled annexin V (Annexin V CF®; Biotium, Fremont, USA) conjugates were prepared following the provided protocols and added to the wells. Additionally, Hoechst (Biotium, Fremont, USA) was introduced into the wells as a nuclear counterstain. The chamber was then placed under a Zeiss AX10 microscope (Zeiss, Jena, Germany), and images of the cells were captured every 30 min over a 24-h time-lapse period. This allowed for the observation of phosphatidylserine translocation, indicated by the movement of apoptotic cells as annexin V conjugates bind to phosphatidylserine on the outer leaflet of the plasma membrane.

### Caspase 3/7 activity

SH-SY5Y cells were seeded onto 6-well plates and allowed to culture for 24 h at 37 °C. Following the culture period, the culture medium was replaced with fresh medium containing a concentration of 25 µM compound **6**. A negative control well with drug-free medium and a solvent control well with an equivalent volume of DMSO were also included in the experiment. After 24 h of incubation with compound **6**, the cells were harvested using a 0.025% trypsin/ethylenediaminetetraacetic acid solution (Sigma-Aldrich, St. Louis, USA). Subsequently, the harvested cells were incubated with CellEvent™ caspase-3/7 green detection reagent (Thermo Fisher Scientific, San Diego, USA), following the manufacturer's instructions. The incubation was carried out at room temperature for 60 min.

Following the incubation period, the apoptotic cells were immediately analyzed using flow cytometry (FACScalibur, BD Biosciences, Erembodegem, Belgium). The resulting data were initially analyzed using FlowJo™ v10 software.[57] Graphs representing the data were generated using GraphPad Prism[58] (Graphpad Software Inc., San Diego, USA). To perform statistical analysis, one-way analysis of variance (ANOVA) followed by Tukey's *t*-test was employed.

### Toxicity assay by *Artemia salina*

The toxicity of compounds **6** and **7** was determined in *Artemia salina* nauplii.[59] Approximately 20 mg of cysts were incubated in 1 L of sterile seawater (Miramar, Brazil) under artificial light at 28 °C. After incubation for up to 48 h, nauplii were collected and added to 96-well plates in which approximately 100 µL of seawater was added to each well along with up to 10 nauplii. Then, the compounds previously diluted in seawater were added to the test wells. The plates were incubated at room temperature for 24 h and the nauplii were counted using a magnifying glass (Zeiss, Jena, Germany), and then the mortality rate was evaluated for each carvacrol derivative tested.

### Irwin test

All experiments were conducted in strict accordance with the ethical guidelines and protocols established by the Ethics and Animal Use Committee (CEUA, Protocol No. 3592221019). The experimental design involved the division of mice into three distinct groups, each consisting of three Swiss mice:

(*i*) G1 control group: these mice received an oral administration of a saline solution.

(*ii*) G2 compound **6** group: these mice were orally administered with 64 mg $kg^{-1}$ of compound **6**, a carvacrol derivative.

(*iii*) G3 high-dose compound **6** group: these mice received an oral dose of 128 mg $kg^{-1}$ of the carvacrol derivative, compound **6**.

After the oral administration of the respective compounds, behavioral parameters, as outlined in Figure 6, were meticulously assessed at specific time intervals, namely 30 min, 1, 2, 3, and 24 h post-administration.

## Supplementary Information

Supplementary information (additional experimental details, $^{1}H$ and $^{13}C$ NMR spectra, and HRMS) and videos S1-S2 are available free of charge at http://jbcs.sbq.org.br.

## Acknowledgments

The authors are grateful for financial support from the Brazilian agencies Conselho Nacional de Desenvolvimento Científico e Tecnológico (CNPq), Coordenação de Aperfeiçoamento de Pessoal de Nível Superior (CAPES), and Universidade Federal da Paraíba (UFPB).

### Author Contributions

A. P. Vasconcelos was responsible for conceptualized the study, performed the biological assays and contributed to manuscript writing; F. J. S. Xavier for conceptualized the study, optimized the synthesis methodology, and processed data; A. Castro for synthesized compounds, contributed to manuscript writing, and reviewed the manuscript; M. F. Lima for conducted fluorescence microscopy assays and participated in manuscript review; L. E. L. Terceiro for performed flow cytometry assays and participated in manuscript review; F. P. L. Silva for optimized the synthesis methodology and processed spectroscopic data; M. L. A. A. Vasconcellos for conceptualized the study, provided supervision, and reviewed the manuscript; B. B. Dantas for supervised the biological assays and reviewed the manuscript; A. M. Barbosa for conducted the *in vivo* assays; S. S. Duarte for contributed to the *in vitro* cytotoxic assays; D. A. M. Araújo for conceptualized the study, provided supervision, and reviewed the manuscript; C. G. Lima-Junior for conceptualized the study, provided supervision, and reviewed the manuscript. All the authors have read and approved the final manuscript.

## References

1. Sung, H.; Ferlay, J.; Siegel, R. L.; Laversanne, M.; Soerjomataram, I.; Jemal, A.; Bray, F.; *CA-Cancer J. Clin.* **2021**, *71*, 209. [Crossref]
2. Lee, Y. T.; Tan, Y. J.; Oon, C. E.; *Eur. J. Pharmacol.* **2018**, *834*, 188. [Crossref]
3. Housman, G.; Byler, S.; Heerboth, S.; Lapinska, K.; Longacre, M.; Snyder, N.; Sarkar, S.; *Cancers* **2014**, *6*, 1769. [Crossref]
4. Blagosklonny, M. V.; *Oncotarget* **2023**, *14*, 193. [Crossref]
5. Dehkordi, A.; Heydarnejad, M. S.; Fatehi, D.; *Oman Med. J.* **2009**, *24*, 204. [Crossref]
6. Lewandowska, A.; Rudzki, G.; Lewandowski, T.; Próchnicki, M.; Rudzki, S.; Laskowska, B.; Brudniak, J.; *Int. J. Environ. Res. Public Health* **2020**, *17*, 6938. [Crossref]
7. Anand, U.; Dey, A.; Chandel, A. K. S.; Sanyal, R.; Mishra, A.; Pandey, D. K.; De Falco, V.; Upadhyay, A.; Kandimalla, R.; Chaudhary, A.; Dhanjal, J. K.; Dewanjee, S.; Vallamkondu, J.; Pérez de la Lastra, J. M.; *Genes Dis.* **2023**, *10*, 1367. [Crossref]
8. Pezzani, R.; *Curr. Top. Med. Chem.* **2022**, *22*, 921. [Crossref]
9. Sharifi-Rad, M.; Varoni, E. M.; Iriti, M.; Martorell, M.; Setzer, W. N.; del Mar Contreras, M.; Salehi, B.; Soltani-Nejad, A.; Rajabi, S.; Tajbakhsh, M.; Sharifi-Rad, J.; *Phytother. Res.* **2018**, *32*, 1675. [Crossref]
10. Fan, K.; Li, X.; Cao, Y.; Qi, H.; Li, L.; Zhang, Q.; Sun, H.; *Anticancer Drugs* **2015**, *26*, 813. [Crossref]
11. Khan, I.; Bahuguna, A.; Kumar, P.; Bajpai, V. K.; Kang, S. C.; *Sci. Rep.* **2018**, *8*, 144. [Crossref]
12. Ahmad, A.; Ansari, I. A.; *Anticancer Agents Med. Chem.* **2021**, *21*, 2224. [Crossref]
13. Jung, C. Y.; Kim, S. Y.; Lee, C.; *Anticancer Res.* **2018**, *38*, 279. [Crossref]

14. Ahmad, A.; Tiwari, R. K.; Saeed, M.; Al-Amrah, H.; Han, I.; Choi, E.-H.; Yadav, D. K.; Ansari, I. A.; *Front. Chem.* **2023**, *10*, 1064191. [Crossref]
15. Azimi, S.; Esmaeil Lashgarian, H.; Ghorbanzadeh, V.; Moradipour, A.; Pirzeh, L.; Dariushnejad, H.; *Med. Oncol.* **2022**, *39*, 253. [Crossref]
16. Alavinezhad, A.; Khazdair, M. R.; Boskabady, M. H.; *Phytother. Res.* **2018**, *32*, 151. [Crossref]
17. Khazdair, M. R.; Boskabady, M. H.; *Respir. Med.* **2019**, *150*, 21. [Crossref]
18. Ghorani, V.; Alavinezhad, A.; Rajabi, O.; Mohammadpour, A. H.; Boskabady, M. H.; *Drug Chem. Toxicol.* **2021**, *44*, 177. [Crossref]
19. Bansal, A.; Saleh-E-In, M. M.; Kar, P.; Roy, A.; Sharma, N. R.; *Molecules* **2022**, *27*, 4597. [Crossref]
20. Silva, F. P. L.; de Assis, P. A. C.; Junior, C. G. L.; de Andrade, N. G.; da Cunha, S. M. D.; Oliveira, M. R.; Vasconcellos, M. L. A. A.; *Eur. J. Med. Chem.* **2011**, *46*, 4295. [Crossref]
21. Faheina-Martins, G. V.; Leite, J. A.; Dantas, B. B.; Lima-Júnior, C. G.; Vasconcellos, M. L. A. A.; Rodrigues-Mascarenhas, S.; Araújo, D. A. M.; *Mediators Inflamm.* **2017**, *2017*, ID 6898505. [Crossref]
22. Xavier, F. J. S.; Lira, A. B.; Verissimo, G. C.; Saraiva, F. S.; de Oliveira Filho, A. A.; de Souza-Fagundes, E. M.; Diniz, M. F. F. M.; Gomes, M. A.; Castro, A. C.; Silva, F. P. L.; Lima-Junior, C. G.; Vasconcellos, M. L. A. A.; *Mol. Diversity* **2022**, *26*, 1969. [Crossref]
23. Lima-Junior, C. G.; Vasconcellos, M. L. A. A.; *Bioorg. Med. Chem.* **2012**, *20*, 3954. [Crossref]
24. Paiva Ferreira, L. A. M.; de Lima, L. M.; Paiva Ferreira, L. K. D.; Bernardo, L. R.; Castro, A.; Lima Junior, C. G.; de Almeida Vasconcellos, M. L. A.; Piuvezam, M. R.; *Mini-Reviews Med. Chem.* **2023**, *23*, 1691. [Crossref]
25. Xavier, F.; Rodrigues, K.; de Oliveira, R.; Lima Junior, C.; Rocha, J.; Keesen, T.; de Oliveira, M.; Silva, F.; Vasconcellos, M.; *Molecules* **2016**, *21*, 1483. [Crossref]
26. Price, K. E.; Broadwater, S. J.; Walker, B. J.; McQuade, D. T.; *J. Org. Chem.* **2005**, *70*, 3980. [Crossref]
27. Robiette, R.; Aggarwal, V. K.; Harvey, J. N.; *J. Am. Chem. Soc.* **2007**, *129*, 15513. [Crossref]
28. Gdovin, M. J.; Kadri, N.; Rios, L.; Holliday, S.; Jordan, Z.; *Semin. Cancer Biol.* **2017**, *43*, 147. [Crossref]
29. Saleem, H.; Iqbal, U.; *Cureus* **2018**, *10*, e2163. [Crossref]
30. Maioral, M. F.; Gaspar, P. C.; Rosa Souza, G. R.; Mascarello, A.; Chiaradia, L. D.; Licínio, M. A.; Moraes, A. C. R.; Yunes, R. A.; Nunes, R. J.; Santos-Silva, M. C.; *Biochimie* **2013**, *95*, 866. [Crossref]
31. Lim, Y. H.; Oo, C. W.; Koh, R. Y.; Voon, G. L.; Yew, M. Y.; Yam, M. F.; Loh, Y. C.; *Drug Dev. Res.* **2020**, *81*, 994. [Crossref]
32. Aydın, E.; Türkez, H.; Keleş, M. S.; *Cytotechnology* **2014**, *66*, 149. [Crossref]
33. Luo, Y.; Wu, J.-Y.; Lu, M.-H.; Shi, Z.; Na, N.; Di, J.-M.; *Oxid. Med. Cell. Longevity* **2016**, *2016*, ID 1469693. [Crossref]
34. Elbe, H.; Yigitturk, G.; Cavusoglu, T.; Baygar, T.; Ozgul Onal, M.; Ozturk, F.; *Ultrastruct. Pathol.* **2020**, *44*, 193. [Crossref]
35. Mari, A.; Mani, G.; Nagabhishek, S. N.; Balaraman, G.; Subramanian, N.; Mirza, F. B.; Sundaram, J.; Thiruvengadam, D.; *Chin. J. Integr. Med.* **2021**, *27*, 680. [Crossref]
36. Bhakkiyalakshmi, E.; Suganya, N.; Sireesh, D.; Krishnamurthi, K.; Saravana Devi, S.; Rajaguru, P.; Ramkumar, K. M.; *Eur. J. Pharmacol.* **2016**, *772*, 92. [Crossref]
37. Sampaio, L. A.; Pina, L. T. S.; Serafini, M. R.; Tavares, D. S.; Guimarães, A. G.; *Front. Pharmacol.* **2021**, *12*, 702487. [Crossref]
38. Falzone, L.; Salomone, S.; Libra, M.; *Front. Pharmacol.* **2018**, *9*, 1300. [Crossref]
39. Ma, Y.-G.; Liu, W.-C.; Dong, S.; Du, C.; Wang, X.-J.; Li, J.-S.; Xie, X.-P.; Wu, L.; Ma, D.-C.; Yu, Z.-B.; Xie, M.-J.; *PLoS One* **2012**, *7*, e37451. [Crossref]
40. Pfeffer, C.; Singh, A.; *Int. J. Mol. Sci.* **2018**, *19*, 448. [Crossref]
41. Kasibhatla, S.; Tseng, B.; *Mol. Cancer Ther.* **2003**, *2*, 573. [PubMed]
42. Reed, J. C.; *Cancer Cell* **2003**, *3*, 17. [Crossref]
43. Carneiro, B. A.; El-Deiry, W. S.; *Nat. Rev. Clin. Oncol.* **2020**, *17*, 395. [Crossref]
44. Raffaghello, L.; Zuccari, G.; Carosio, R.; Orienti, I.; Montaldo, P. G.; *Clin. Cancer Res.* **2006**, *12*, 3485. [Crossref]
45. Lakhani, S. A.; Masud, A.; Kuida, K.; Porter, G. A.; Booth, C. J.; Mehal, W. Z.; Inayat, I.; Flavell, R. A.; *Science* **2006**, *311*, 847. [Crossref]
46. Daina, A.; Michielin, O.; Zoete, V.; *Sci. Rep.* **2017**, *7*, 42717. [Crossref]
47. Lipinski, C. A.; Lombardo, F.; Dominy, B. W.; Feeney, P. J.; *Adv. Drug Delivery Rev.* **2012**, *64*, 4. [Crossref]
48. Veber, D. F.; Johnson, S. R.; Cheng, H.-Y.; Smith, B. R.; Ward, K. W.; Kopple, K. D.; *J. Med. Chem.* **2002**, *45*, 2615. [Crossref]
49. Ali, J.; Camilleri, P.; Brown, M. B.; Hutt, A. J.; Kirton, S. B.; *J. Chem. Inf. Model.* **2012**, *52*, 420. [Crossref]
50. Ntungwe N, E.; Domínguez-Martín, E. M.; Roberto, A.; Tavares, J.; Isca, V. M. S.; Pereira, P.; Cebola, M.-J.; Rijo, P.; *Curr. Pharm. Des.* **2020**, *26*, 2892. [Crossref]
51. Kachenton, S.; Jiraungkoorskul, W.; Kangwanrangsan, N.; Tansatit, T.; *Environ. Sci. Pollut. Res.* **2019**, *26*, 14706. [Crossref]
52. Thiagarajan, V.; Seenivasan, R.; Jenkins, D.; Chandrasekaran, N.; Mukherjee, A.; *Aquat. Toxicol.* **2020**, *225*, 105541. [Crossref]
53. Cibulski, S.; Teixeira, T. F.; Varela, A. P. M.; de Lima, M. F.; Casanova, G.; Nascimento, Y. M.; Fechine Tavares, J.; da Silva, M. S.; Sesterheim, P.; Souza, D. O.; Roehe, P. M.; Silveira, F.; *Vaccine* **2021**, *39*, 571. [Crossref]

54. Pecoraro, R.; Scalisi, E. M.; Messina, G.; Fragalà, G.; Ignoto, S.; Salvaggio, A.; Zimbone, M.; Impellizzeri, G.; Brundo, M. V.; *Microsc. Res. Tech.* **2021**, *84*, 531. [Crossref]
55. Campbell, D. E. S.; Richter, W.; *Acta Pharmacol. Toxicol.* **1967**, *25*, 345. [Crossref]
56. Mathiasen, J. R.; Moser, V. C.; *Curr. Protoc. Pharmacol.* **2018**, *83*, [Crossref]
57. *BD Life Sciences FlowJo™*, version 10; Becton, Dickinson and Company, Franklin Lakes, NJ, USA, 2023.
58. *GraphPad Prism*, version 10.0.0; GraphPad Software, Boston, MA, USA, 2023.
59. Sorgeloos, P.; Remiche-Van Der Wielen, C.; Persoone, G.; *Ecotoxicol. Environ. Saf.* **1978**, *2*, 249. [Crossref]

*Submitted: December 4, 2023*
*Published online: February 16, 2024*